URSI GASS 2020, Rome, Italy, 29 August- 5 September 2020

First Principle Scintillation Characterization of Natural and Artificial Disturbances on V/W Band Signals in the Ionosphere Using the Multiple Phase Screen Technique

Andrew J. Knisely[(1)], and Andrew J. Terzuoli[(1)]
(1) Institute of Electrical & Electronics Engineers (IEEE), USA

Abstract

The V/W frequency band (75GHz to 110 GHz) is in current interest for application to modern 5G networks that rely on the SATCOM infrastructure to support long range mobile communications. The environmental effects on a V/W band signal in this frequency range must be analyzed to establish an expectation in regards to signal quality and sustainability. In particular Ionospheric disturbances caused by geomagnetic storms and High Altitude Nuclear Explosions (HANES) is the primary focus of this paper. The results demonstrate that the V/W bands are generally sustainable in geomagnetic storms. The scintillation index has an order of magnitude of 10^{-3} for each frequency tested in a Multiple Phase Screen (MPS) model. The HANE experiment conducted with a computational plasma physics model demonstrates significant signal disturbances in the initial 45 seconds of the blast as the burst occurs in direct line-of-sight to the transmitter. The signal recovery depends greatly on the Ionosphere's ability to return to a steady state after the occurrence of a HANE.

1 Introduction

A disturbance to the Ionosphere can cause a change in the distribution of the electron content. A common natural occurrence that can contribute to this alteration are geomagnetic storms. Geomagnetic storms result from a compression of the magnetosphere due to the arrival a solar wind discontinuity. The electric fields, currents, and particle precipitation increase as a large amount of energy is deposited into the Ionosphere. The auroral E-region electron densities increase in conjunction with ion and electron temperatures at high latitudes. At mid-latitudes, the wind speeds increase and drive the F region plasma toward higher altitudes which can result in ionization enhancements. For big storms, the enhanced neutral winds and composition changes penetrate toward the equatorial region [1].

High Altitude Nuclear Explosions (HANES) contribute an extraordinary amount of energy to the Ionosphere. Up to 3/4 of the energy yielded by the nuclear explosion may be expended in ionizing the atmosphere, resulting in changes that are characteristic of the burst and the debris altitude. Nuclear explosions at high altitudes may affect a considerable portion of the Ionosphere in a manner similar to solar activity, however, the mechanisms of the interactions with the atmosphere are quite different. Due to the complexities of these interactions, descriptions of the typical changes to be expected from a nuclear explosion are often not applicable or very meaningful without explicit statements of the conditions [2].

During a nuclear explosion, the air inside the fireball is at a temperature of many thousands of degrees. Electron density and collision frequency are high in addition to absorption of electromagnetic waves. The regions around the fireball is ionized in varying degrees by the initial thermal and nuclear radiations and by the delayed particles from the radioactive debris. As the detonation altitude increases, the radiation can escape at greater distances and the electron density will reach values at which electromagnetic signal propagation can be affected. In the D region of the Ionosphere, the most persistent absorption of electromagnetic waves will take place. In the E and F regions, the frequency of particle collisions is low, and refraction is the predominant effect [2].

The Ionosphere behavior, in general, can be described as a plasma. The local electric field (E-field) governs the movement of the plasma and the particle is also a source of the electric field. Electrons typically respond much more rapidly to an E-field and ion-motion can be neglected. A group of electrons in the plasma will move in response to the wave field. This movement alters the local concentration of the electric charge, thereby making their own contribution to the electric field. [3]

Computationally modeling the fluctuations of electron density in the Ionosphere caused by natural and artificial disturbances typically involves the use of phase screens. A multiple phase screen model compresses the thick Ionosphere layer into a series of thin screens that sample the irregularities on a finite grid. This method avoids the computational limitations of discretizing a large layer while calculating the E-field at high frequencies. A metric to measure the effects of randomized Ionosphere irregularity fluctuations is the scintillation index. The scintillation index is the normalized variance of intensity fluctuations defined in formula (1). The variable "I" is the intensity calculated from the absolute square of the electric field, i.e.

$$S_4 = \sqrt{\frac{\langle I^2 \rangle - \langle I \rangle^2}{\langle I \rangle^2}} \qquad (1)$$

The following section describes the process of developing the multiple phase screen model and the test cases for examining first principle signals transmitted in V/W frequency bands.

2 Methodology

The Multiple Phase Screen (MPS) model begins with defining the parameters of each phase screen. The phase screen converts the fluctuations of electron density into a phase variance and power spectral density in the spatial frequency domain. The grid length of the phase screen is dictated by the outer scale (largest) of the irregularities while the sample index is dictated by the inner scale (smallest) of the irregularities. The outer and inner scale sizes are chosen on the order of kilometers and meters, respectively, as often found in literature (see [4]). Table I. summarizes these phase screen parameters.

Table 1. Phase Screen Parameters

Parameter:	Value
L: Grid Length [km]	10 L_o
L_o : Outer Scale [km]	3
l_i : Inner Scale [meters]	150
N: Spatial Samples	4096

A total of five phase screens are used in this MPS model. The region between each phase screen is considered free space. The propagation through free space is accomplished using the split-step Fourier method, also known as the spectral method. The spectral method solves the paraxial approximation of the scalar Helmholtz equation to relax the phase sampling requirements and ease the computational expense of high frequency wave propagation. This is also known as the parabolic wave equation (2), given by

$$\frac{\partial \underline{U}(x,z)}{\partial z} = \frac{1}{2\underline{\gamma}} \frac{\partial^2 \underline{U}(x,z)}{\partial x^2} \tag{2}$$

Where "U" is the amplitude and γ is the propagation constant of the wavefront consisting of the attenuation parameter set equal to zero and the propagation constant equal to $2\pi/\lambda$. The formulation for the parabolic wave equation is written as an interior problem with natural boundary conditions is

$$BC \qquad \begin{cases} \underline{U}(0,z) = 0 \\ \underline{U}(L,z) = 0 \end{cases} \qquad 0 \le z \le Z_{\max}$$

$$IC \qquad \underline{U}(x,0) = \underline{\phi}(x) \qquad 0 \le x \le L$$

Where "$\underline{\phi}$(x)" is the initial input function, "L" is the grid length of the wavefront samples, and "z" is the distance along the propagation path with respect to altitude.

The spectral method technique relies on transforming from spatial position to spatial frequency domains and using trigonometric global basis functions to approximate the continuous PDE defined in (2). The derivative is approximated by the sequence of Fourier modes in the following manner:

$$\frac{d^k U_N}{dx^k}(x_j) = \sum_{|n| \le N} (in)^k \hat{a}_n e^{\left[\frac{2\pi i}{L}\right] n(x_j)} \tag{3}$$

The Fast Fourier transform is taken to acquire the Fourier *U* coefficients, $\hat{a}_n$ via

$$\hat{a}_n = \text{fft(U)} = \frac{1}{N} \sum_{j=0}^{N-1} U(x_j) e^{inx_j} \tag{4}$$

The second order spatial derivative is formulated into a square diagonal matrix where each dimensional length is equal to the length of the input vector. The sequence of Fourier modes are arranged to be evenly uniform across the spatial *x* grid. Applying this process, take the Fourier transform on both sides of the parabolic wave equation:

$$\int_{-\infty}^{\infty} \left[\frac{\partial^2 \underline{U}(x,z)}{\partial x^2} \right] e^{-\beta x} dx = 2\underline{\gamma} \int_{-\infty}^{\infty} \left[\frac{\partial \underline{U}(x,z)}{\partial z} \right] e^{-\beta x} dx \tag{5}$$

This forms an ODE in the spatial frequency domain, i.e.

$$-K^2 \widetilde{\underline{U}}(K,z) = 2\underline{\gamma} \frac{\partial \widetilde{\underline{U}}(K,z)}{\partial z} \tag{6}$$

Integrating both sides of the equation yields

$$\int_{z_1}^{z_2} -\frac{K^2}{2\underline{\gamma}} dz = \int_{z_1}^{z_2} \frac{1}{\widetilde{\underline{U}}(\mathrm{K},z)} d\widetilde{\underline{U}}(\mathrm{K},z) \tag{7}$$

The solution is then inverse Fourier transformed back to the spatial position domain, i.e.

$$\widetilde{\underline{U}}(\mathrm{K},z_2) = \widetilde{\underline{U}}(\mathrm{K},z_1) e^{-\left(\frac{K^2}{2\underline{\gamma}}\right)\Delta z} \tag{8}$$

$$\underline{U}(x,z_2) = ifft\left(\widetilde{\underline{U}}(x,z_1)\right) \tag{9}$$

The number of phase screens is dictated by adequate sampling of this free space when using the spectral method. The minimum frequency examined in this paper includes 378 MHz. By using this frequency and a distance of 380 km between each screen, the free space sampling requirement can be verified by

$$\Delta z < \frac{2L\Delta x}{\lambda}$$

$$\rightarrow 380000 < \frac{2(30000)\left(\frac{30000}{4096}\right)}{\left(3\times10^{8}/378\times10^{6}\right)}$$

$$\rightarrow 380000 < 553710$$

Figure 1 illustrates the MPS model along with a superimposed electron density distribution whose density variances are assigned to a respective phase screen.

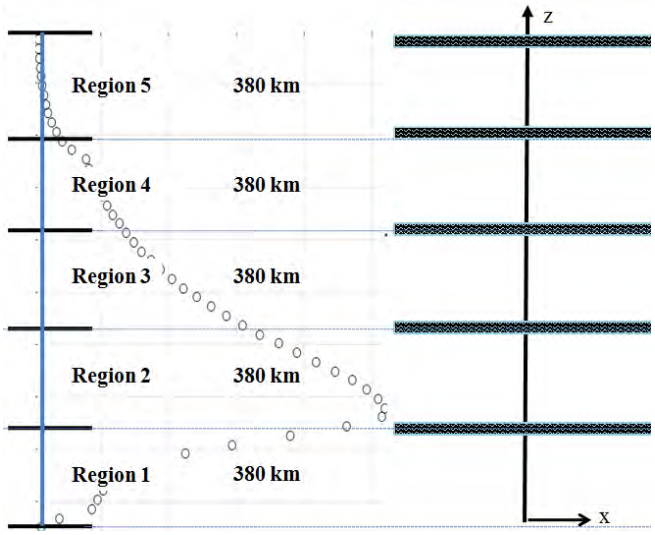

Figure 1. MPS Layout

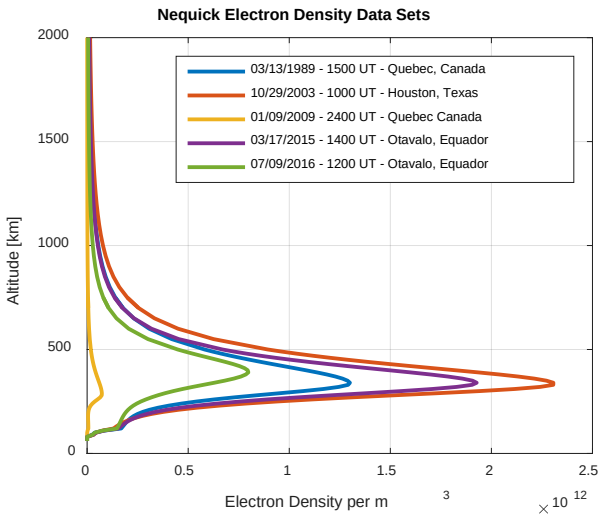

Figure 2. Electron Density Distributions

The test cases collected for the natural disturbance analysis for V/W band signals is shown in Figure 2. The electron density data collection was acquired from NeQuick, an online database. NeQuick is a three-dimensional and time dependent Ionosphere electron density model based on an empirical climatological representation of the Ionosphere [5].

Figure 3 shows a sequence of an electron density distribution data set acquired after a computationally modeled nuclear detonation. The data is acquired from a plasma physics based software.

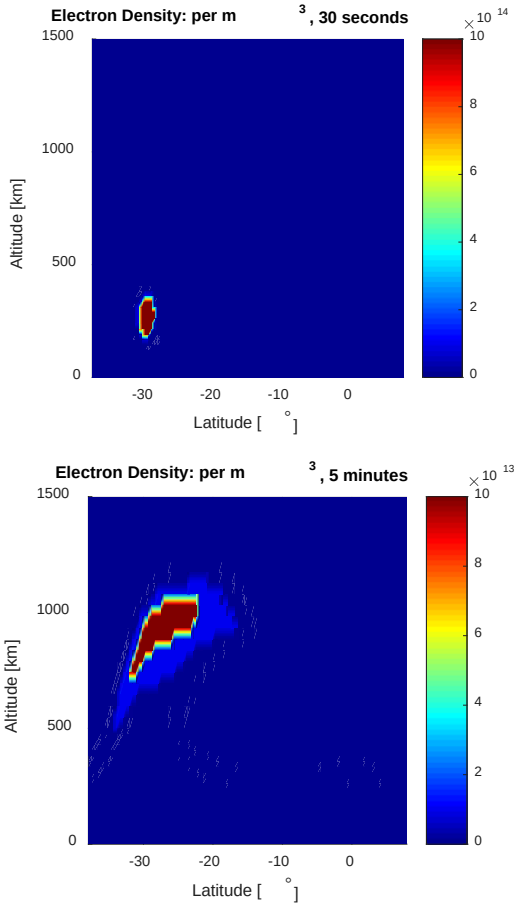

Figure 3. Nuclear Detonation Electron Density Distribution: 30 seconds after (top) and 5 minutes after (bottom)

The MPS simulations in this paper are conducted at the frequencies of 378 MHz, 40 GHz, 72 GHz, 84 GHz, and 96 GHz. The following section shows the resulting scintillation calculations from these MPS simulations. Each signal generated from the transmitter has an initial amplitude of unity and a phase of zero. The E-field is considered to be a uniform plane wave prior to phase screen incidence.

3 Results

Figures 4 and 5 show a significant difference between the low frequency and high frequency scintillation behavior of the signal. At 378 MHz, the scintillation saturates close to unity during the more severe geomagnetic storms. At 84 GHz, the scintillation is much less insignificant, only on the order of 10^{-3}.

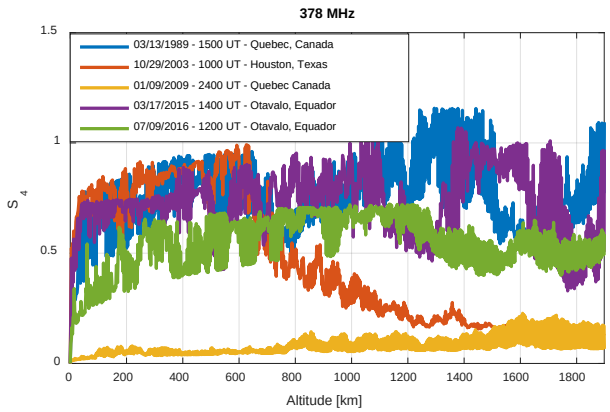

Figure 4. Scintillation Curve for 378 MHz signal

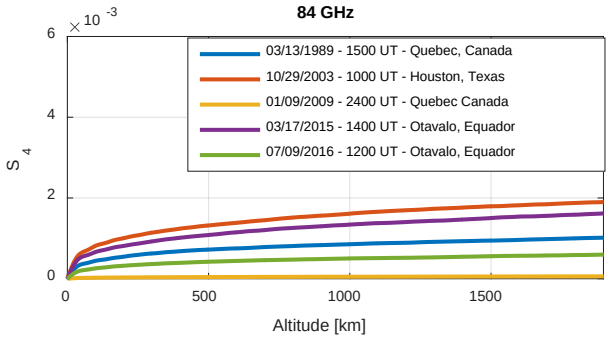

Figure 5. Scintillation Curve for 378 MHz signal

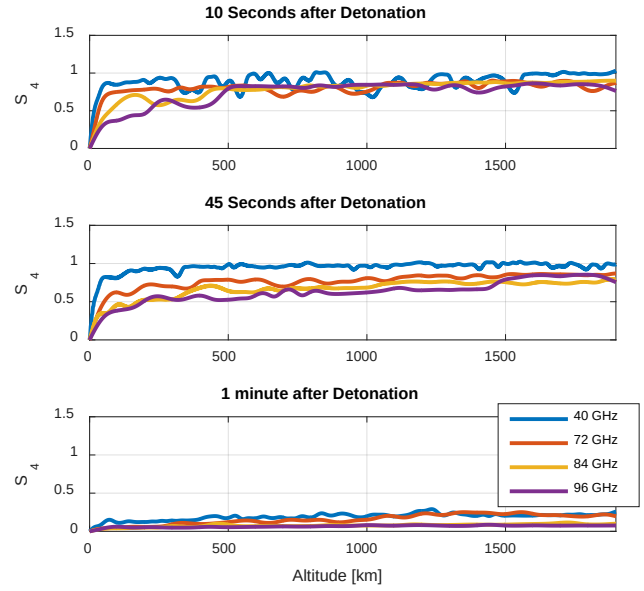

Figure 6. Scintillation Curve Time Sequence after Nuclear Detonation

The HANE results show that V/W band signals are greatly impacted by the excitation of the electron content in the Ionosphere after a nuclear detonation. The significant scintillation occurs in the initial 45 seconds of the blast and begins to settle after 1 minute. The electron density content is high enough to yield a large phase variance when converting the electron density to the power spectrum. The larger power spectrum results in a greater magnitude output from the phase screen realization, thus interfering greatly to the intensity of the E-field. It should be noted that the model is considered first principle as many of the equations used to represent phases of the nuclear detonation are based on generalized descriptions involving nuclear and plasma physics phenomenon.

4 Conclusion

The results demonstrate that the environmental factors in the Ionosphere must be considered in extreme cases of electron density fluctuations caused by Ionosphere disturbances Even though the geomagnetic storms yielded little impact on a V/W band signal, a HANE event has significant impact. Future research will demonstrate the temporal impact of such events on a wideband signal that incorporate the multiple phase screen techniques to simulate ionic effects. The correlation between phase change and time delay must be understood for HANE events. The significance of these results will lead to a model that can assist with the design of assured communication systems

5 Acknowledgements

We would like to thank our research assistants for their continued dedication and support on this research effort.

6 References

[1] R.W. Schunk, "Ionospheres: Physics, Plasma Physics, and Chemistry", Cambridge University Press, Cambridge, UK, 2000.

[2] Samuel Glasstone, and Philip J. Dolan, "The Effects of Nuclear Weapons", United States Department of Defense and the Energy Research and Development Administration, Washington, D.C., 1977.

[3] R.0. Dendy, "Plasma Dynamics", Oxford Science Publications, Clarendon Press, 1990.

[4] Dennis L Knepp, "Propagation of Wide Bandwidth Signals Through Strongly Turbulent Ionized Media", electronic file available at: https://apps.dtic.mil/dtic/tr/fulltext/u2/a131355.pdf, 1982.

[5] Nava, B., P. Coisson and S.M. Radicella, “A New Version Of The NeQuick Ionosphere Electron Density Model”, Journal of Atmospheric and Solar-Terrestrial Physics, doi:10.1016/j.jastp.2008.01.015.